Nuclear Instruments and Methods in Physics Research A 350 (1994) 174–183
North-Holland

NUCLEAR INSTRUMENTS & METHODS IN PHYSICS RESEARCH
Section A

Threshold Cherenkov detectors for a meson trigger in a magnetic spectrometer

D. Miśkowiec, E. Grosse, P. Senger[1], W. Waluś
Gesellschaft für Schwerionenforschung m.b.H, D-64 291 Darmstadt, Germany

Received 23 March 1994; revised form received 9 June 1994

Lucite and water Cherenkov detectors were built for a magnetic spectrometer (KaoS at SIS). The task of the detectors is to improve the proton suppression at the trigger level in experiments on meson production from nuclear collisions. By applying Polyphenyl 1 as wavelength shifter addition to water a light yield increase by a factor of 2 was achieved. Material with a very high reflectance (better than that of Teflon) was tested and applied as a wall covering for the water detectors. The efficiency of the detectors was measured as a function of the particle velocity, and the data were compared to formulae for Cherenkov light emission and detection.

1. Introduction

Relativistic nucleus–nucleus collisions offer the unique possibility to produce and to study hot and dense nuclear matter in the laboratory. Meson production has been established as an important probe of the dynamics of high baryon and energy densities in heavy ion reactions [1]. In particular subthreshold K^+ production is expected to be sensitive to nuclear matter properties at increased density [2]. The laboratory kinetic energy needed to produce a K^+ in a free NN-collision is 1.58 GeV. In heavy ion collisions around 1 GeV/nucleon K^+ production proceeds preferentially through a two-step mechanism ($NN \rightarrow N\Delta$, $N\Delta \rightarrow K^+\Lambda N$) which is likely to be density dependent. In addition, the small final state interaction of K^+ with the surrounding matter makes positive kaons an especially advantageous probe.

In order to measure differential cross section for subthreshold K^+ production in heavy ion collisions a double focusing magnetic spectrometer [3] was designed and installed at the heavy ion synchrotron SIS in Darmstadt (Fig. 1). The spectrometer is optimized to measure the rare K^+ mesons in the high background of pions and protons. Its compact size – the distance between target and focal plane is less than 7 m – minimizes the loss of kaons due to decay in flight. A large angular acceptance up to 35 msr and a momentum range of $p_{max}/p_{min} \approx 2$ up to $p_{max} = 1.8$ GeV/c permit the measurement of kaon momentum and angular distributions with high efficiency; a selective kaon trigger is needed to make use of the high beam intensity of SIS. The identification of particles in the spectrometer is done by measuring their momentum and time of flight (TOF). Segmented plastic scintillator TOF start and stop detectors are placed between the quadrupole and dipole and at the focal plane of the spectrometer, respectively. Two multiwire proportional chambers (MWPC) for particle tracking are located between the exit of the dipole magnet and the focal plane. An event characterization is performed with two highly granulated plastic scintillator arrays covering angles from 0.5° to 10° and from 12° to 48°, which measure the spectator fragments and charged particles at midrapidity, respectively. This information is used to determine the orientation of the reaction plane and the centrality of the collision [4].

The proton and pion background is the main problem in measuring kaons at SIS energies. In a typical KaoS experiment (Au + Au at 1 GeV/nucleon) one observes per one kaon about 10000 protons and 400 pions which thus have to be suppressed at the trigger level. A simple hardware TOF trigger is generated by a coincidence between any of the start and any of the stop paddles. By adjusting the timing one can suppress protons and pions by a factor of 10 to 1000, depending on the TOF difference and hence on the momentum of the particles. For high particle momenta this difference decreases and the TOF discrimination at the hardware trigger level is not possible anymore. Threshold Cherenkov detectors may be used at these higher momenta to tag the fast mesons and thus to suppress protons at the trigger level. The pion yield, on the other hand, decreases with increasing momentum and thus contributes only moderately to the trigger rate.

[1] Corresponding author. Tel. +39 (6151) 359-0, fax +39 (6151) 359-785, e-mail senger@vsbx.gsi.de.

SSDI 0168-9002(94)00690-9

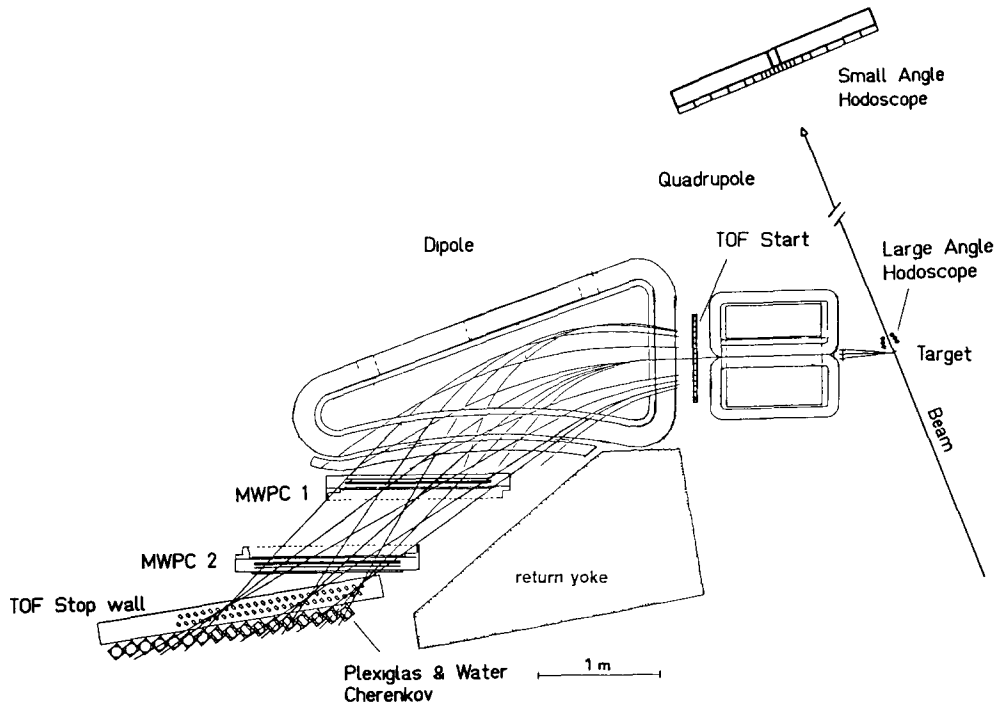

Fig. 1. The Kaon Spectrometer (KaoS) at SIS with its detector system: TOF start detector between the quadrupole and the dipole, TOF stop detector along the focal plane (both consisting of plastic scintillators), two multiwire proportional chambers (MWPC) for tracking, lucite and water Cherenkov detectors for suppressing protons, two hodoscopes for event characterization (at the target and 7 m downstream).

A row of threshold Cherenkov counters for proton suppression is placed behind the TOF stop wall. It consists of ten lucite ($n = 1.49$) and six water ($n = 1.34$) modules which have velocity thresholds of $\beta_C = 0.67$ and $\beta_C = 0.75$, respectively. The lucite detectors cover the low momentum part of the focal plane while the water detectors are located at its high momentum end. The detectors are oriented perpendicularly to the central trajectories. This arrangement requires some overlap of the modules, as shown in Fig. 1.

Within a momentum range of 550 MeV/c < p < 1000 MeV/c kaons are fast enough to produce Cherenkov light in the lucite and water radiators whereas protons have velocities lower than the Cherenkov thresholds. Thus a triple coincidence "TOF start & TOF stop & lucite or water Cherenkov" defines a meson (pion or kaon) trigger.

2. Design studies and tests

In order to detect particles above the Cherenkov threshold with a maximum efficiency and to suppress particles below threshold the detectors have to fulfill the following requirements: a) high Cherenkov light yield, b) low dependence of the light yield on the particle position and angle of incidence and c) low scintillation light yield. We tried out several materials as Cherenkov radiators and tested various light collection systems. The final versions of the detectors were constructed taking into account the results of the tests which are described in this section.

2.1. Test method

Cosmic rays with $Z = 1$ and $\beta \simeq 1$ are an excellent tool to test the light yield of Cherenkov radiators and light collection systems. We used a setup of plastic scintillators ($10 \times 5 \times 1$ cm^3) to trigger on cosmic rays and to measure the Cherenkov light output as a function of the position of impact (Figs. 2a and 2b). The position was determined with an accuracy of 5 cm by coincidence and anticoincidence requirements between the plastic scintillators. The associated electronics setup is shown in Fig. 2c. The external triggering allowed to observe even very small signals of the tested detector.

The muon peak position in the ADC spectrum depends on the voltage supplied to the photomultiplier and thus is not a good measure of the light yield. Therefore, we used the average number of photoelectrons N_{phe} which reach the first dynode of the photo-

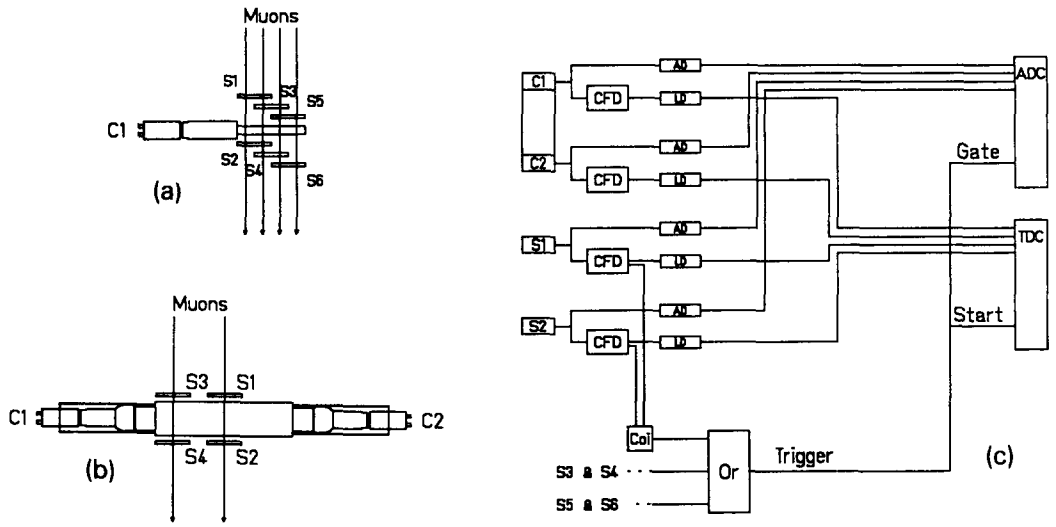

Fig. 2. The setups used to test the light yield of Cherenkov detectors with cosmic rays: (a) 20 cm detector; (b) 40 cm detector; (c) electronics. Plastic scintillators S1–S6 were used to produce a cosmic ray trigger and to define the position of impact. Photomultiplier signals from the tested detector (C1,C2) and those from the six trigger detectors (S1... S6) were digitized in CAMAC ADCs and TDCs. CFD, AD and LD mean constant fraction discriminator, analog delay and logic delay respectively.

multiplier to describe the light yield of the tested detectors. The number of photons hitting the photocathode and the number of electrons emitted from the first dynode are higher than the number of photoelectrons and thus the stage between the photocathode and the first dynode is the statistical "bottle-neck" of the photomultiplier. The distribution of the actual number of photoelectrons n around its mean value N_{phe} is described by the Poisson statistics:

$$p(n) = \exp(-N_{\mathrm{phe}})\frac{(N_{\mathrm{phe}})^n}{n!}. \tag{1}$$

The Poisson distribution has a maximum between N_{phe} and $N_{\mathrm{phe}} - 1$ and a standard deviation $\sigma = \sqrt{N_{\mathrm{phe}}}$. The theoretical detection efficiency is limited to $p(n > 0) = 1 - \exp(-N_{\mathrm{phe}})$, whereas the real efficiency $p(n > n_{\mathrm{min}})$ is lower and depends on the discrimination threshold n_{min}.

There are several methods to extract N_{phe} from the cosmic ray energy loss spectrum.

(i) The first method requires the knowledge of the single photoelectron peak and the ADC pedestal (which corresponds to zero photoelectrons) positions. The mean photoelectron number can then be expressed as the ratio of the cosmic ray peak position to the single photoelectron peak position, both measured from the pedestal:

$$N_{\mathrm{phe}} = \frac{X_{\mathrm{c}} - X_0}{X_{1\,\mathrm{phe}} - X_0}, \tag{2}$$

where X_{c}, X_0 and $X_{1\,\mathrm{phe}}$ are the ADC spectrum positions of the cosmic ray peak, the pedestal and the single photoelectron peak, respectively. The uncertainty of the single photoelectron peak position and the nonlinearity of the photomultiplier are the main sources of systematic errors.

(ii) If the light output is very low (on the order of several photoelectrons), the ratio of the pedestal content to the total can be used:

$$N_{\mathrm{phe}} = -\ln(S_0/S), \tag{3}$$

where S_0 is the number of counts accumulated in the ADC pedestal and S is the total number of counts in the whole spectrum (i.e. the number of triggers). Of course, the acquisition has to be triggered externally and one has to make sure that the pedestal does not contain counts generated by false triggers.

(iii) The cosmic ray peak position X_{c} and its width σ_{c} can be used to calculate N_{phe}:

$$N_{\mathrm{phe}} = \left(\frac{X_{\mathrm{c}} - X_0}{\sigma_{\mathrm{c}}}\right)^2. \tag{4}$$

However, since the plastic scintillators which define the trigger have finite sizes, the contribution of the inclined trajectories shifts the muon peak in the ADC spectrum of the tested detector towards higher ADC values and makes it broader. In order to estimate the associated systematic error of N_{phe} we performed a simple Monte Carlo simulation. The effect becomes significant for high light yields (see Table 1). Knowing the geometry, one can calculate the necessary correction. The N_{phe} value calculated via Eq. (4), even when not corrected, can be used as the lower bound for the true N_{phe}.

Another way to avoid the additional broadening of the peak is described in Ref. [5]. There a light diode

Table 1
Simulation of the light yield taking into account finite inclination angles of the cosmic rays caused by the finite size of the trigger detectors. The calculation is based on the test setup (Fig. 2b) and on Eq. (4). The active area of the trigger detectors is 5 cm × 10 cm and the distance between them is 20 cm. The first two columns show the yield N_{phe} and the width FWHM assuming that the cosmic rays traverse the detector perpendicularly to its front surface ($\alpha = 0$). The columns 3 and 4 show the peak position X_c and the width $FWHM_c$ for finite angles of incidence ($\alpha \geq 0$). The number of photoelectrons $N_{phe\,c}$, calculated from X_c and $FWHM_c$ according to Eq. (4), is given in column 5. All values are in photoelectrons

$\alpha = 0$ N_{phe}	$\alpha = 0$ FWHM	$\alpha \geq 0$ X_c	$\alpha \geq 0$ $FWHM_c$	$\alpha \geq 0$ $N_{phe\,c}$
10.0	7.4	10.3	7.4	10.6
100.0	23.6	102.6	24.4	98.5
200.0	33.3	205.2	35.5	185.3
1000.0	74.5	1026.0	96.9	621.8

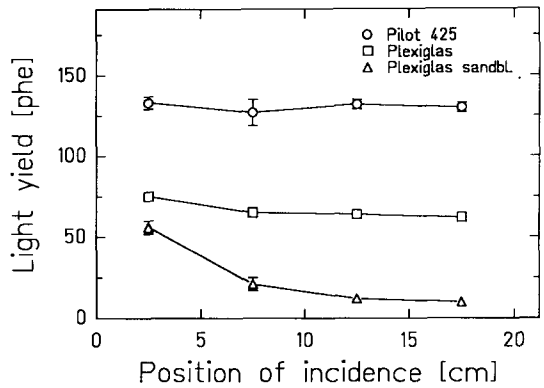

Fig. 3. Light yield (in photoelectrons) of three different lucite radiators as a function of the hit position. The position is measured from the end of the radiator at which the photomultiplier is coupled. The bars represent the relative errors. The uncertainty related to the absolute yield determination is about 30%.

was used to generate a peak at the same position and with the correct width.

(iv) A very rough but simple method is to watch both single photoelectron and cosmic ray signals on the oscilloscope screen and to estimate their surfaces which correspond to electric charges. The ratio of this two surfaces gives the number of photoelectrons.

The first and the third methods were used to determine the number of photoelectrons for the tested detectors.

2.2. Lucite Cherenkov detector

The simplest lucite Cherenkov detector is just a piece of lucite wrapped in aluminum foil and coupled to a photomultiplier. The light collection in this case is mainly due to total internal reflection in the radiator. The light collection efficiency depends thus on the angle of incidence and the velocity of the particle producing the Cherenkov light. For example, the Cherenkov photons produced by normally incident pions of 600 MeV/c have an opening angle of 47° and thus are guided by subsequent total reflections to the ends of the radiator, while the light produced by kaons of the same momentum (Cherenkov opening angle of 30°) would leave the radiator and would be reflected by the aluminum foil only. We considered the use of wavelength shifter and rough diffuse walls in order to get rid of this effect. We tested three detector prototypes: Pilot 425 [6] and Plexiglas GS 218 [7], both polished and wrapped in Teflon, and Plexiglas GS 218 with sandblasted and painted walls. All pieces were 20 cm long, 5 cm wide and 2.5 cm high. Pilot 425 is lucite with an addition of wavelength shifter [8]. The wavelength shifter increases the light yield in the wavelength range which is accepted by photomultipliers and partially removes the correlation between the directions of the particle and photons, since the emission of photons converted by the wavelength shifter is isotropic. The 2 in. photomultipliers EMI 9914B [9] or EMI 9954QB (quartz window) were coupled with optical grease to one end of each radiator module.

The light yield of these three samples for cosmic rays is presented in Table 2. The number of photoelectrons was determined using the position of the single photoelectron peak (Eq. (2)). The dependence of the yield on the particle position of impact is presented in Fig. 3. The sandblasted walls had to be excluded from further considerations because of the large position dependence of the light output. The Pilot 425 yielded 1.7 times more light than the Plexiglas sample. In order to measure the response for subthreshold particles these two detectors, both wrapped in Teflon, were additionally tested using protons and pions with momenta analyzed by the magnetic spectrometer SPES3 at SATURNE. The Plexiglas radiator turned out to have a much more pronounced threshold effect which is in agreement with other reports [10,11]. We therefore decided to use Plexiglas GS 218 as a radiator material. The detector in its final version (described in Section 3) yields 35 ± 7 photoelectrons for cosmic rays. The light output from both ends of the radiator and the summed signal spectra for cosmic rays incident approximately in the middle of the detector are shown in Fig. 4. The position dependence of the yield is shown in Fig. 5.

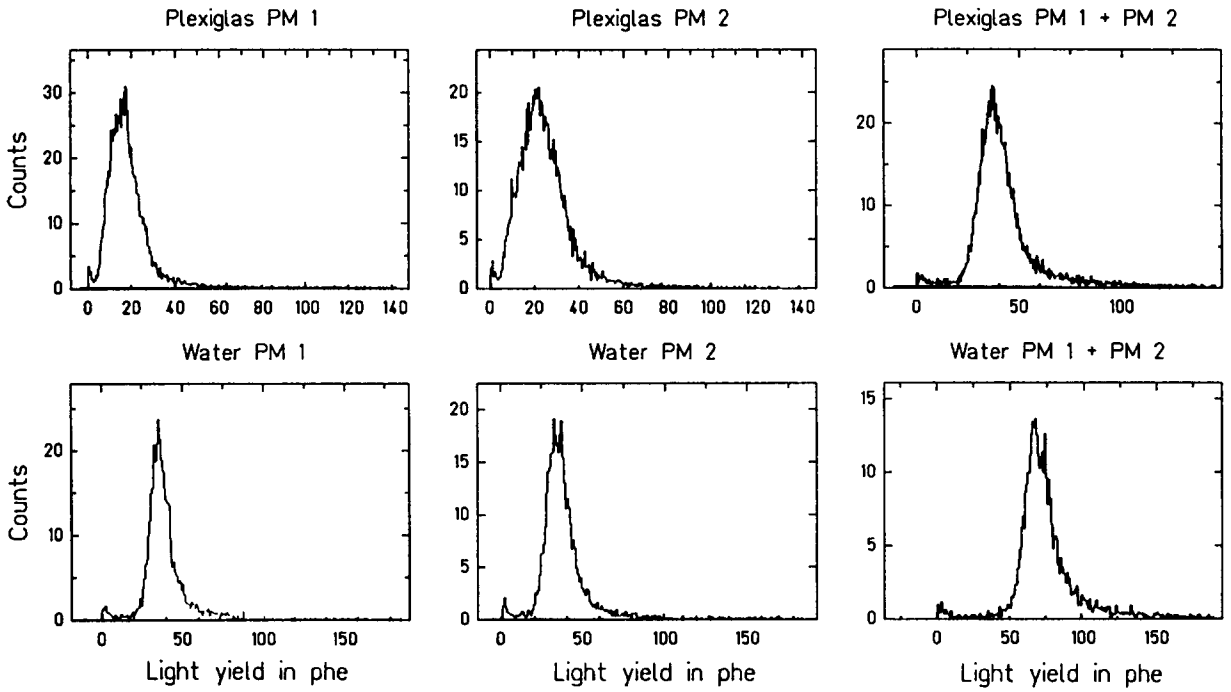

Fig. 4. Charge spectra (in photoelectrons) of both photomultiplier signals and their sum, accumulated with cosmic rays hitting approximately the centre of the detector for lucite and water Cherenkov modules in their final versions.

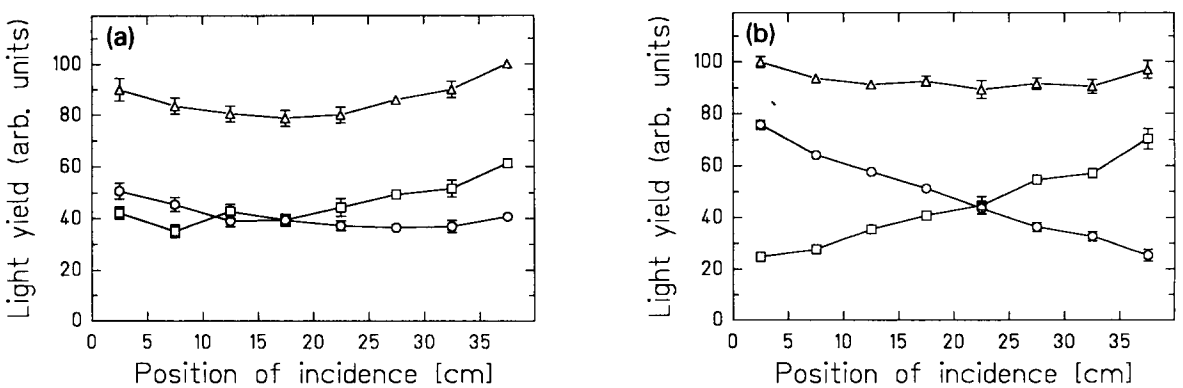

Fig. 5. Light yield (in arbitrary units) of (a) lucite and (b) water Cherenkov detectors (final version) as a function of the particle position of impact. The signals of both photomultipliers (circles and squares) as well as their sum (triangles) are presented.

Table 2
Cherenkov light yield from different plastic radiators. All samples had dimensions 2.5 × 5 × 20 cm^3 and were read out from one end by a 2 in. EMI glass-window photomultiplier

Type of radiator	Yield in photoelectrons
Plexi bare (only total internal reflection)	44 ± 12
Plexi wrapped in 4 layers of 0.1 mm Teflon	67 ± 10
Pilot 425 bare (only total internal reflection)	60 ± 6[a]
Pilot 425 wrapped in 1 layer of aluminum foil	89 ± 9[a]
Pilot 425 wrapped in 1 layer of 0.1 mm Teflon	92 ± 9[a]
Pilot 425 wrapped in 4 layers of 0.1 mm Teflon	118 ± 10
Pilot 425 wrapped in 8 layers of 0.1 mm Teflon	128 ± 11[a]
Plexi sandblasted and painted with scintillator paint NE 560	7.3 ± 2

[a] The absolute number of photoelectrons was calculated by normalizing to the light yield for 4 layers of Teflon (118 photoelectrons)

2.3. Water Cherenkov detector

Similarly as in the case of lucite, the good transparency of water allows to use the radiator itself to collect the produced photons. The test module consisted of an aluminum box (10 × 10 × 25 cm^3, wall thickness 2 mm) filled with deionized water. Two EMI 9821B 3 in. photomultipliers were mounted at both ends of the detector. The test detector was used to investigate different kinds of diffuse reflecting wall coverings. The Immobilon-P Transfer Membrane [12], which is hydrophobic and retains its good reflectance also in contact with water, proved to be an even better reflector material than thick Teflon (Table 3). Furthermore, several wavelength shifters were studied in order to increase the light yield in the wavelength range where glass window photomultipliers are sensitive. Only one of them, Polyphenyl 1 [13], proved to be easily soluble in water. Another one, p-Terphenyl [13], could be solved in small concentrations in warm water. The light yield dependence on the wavelength shifter concentration is presented in Fig. 6. The addition of 8 ml/l Polyphenyl 1 increased the light yield by a factor of two. We decided, therefore, to use deionized water with an addition of 8 mg/l Polyphenyl 1 as radiator and Immobilon-P as wall covering. The final detector (Section 3) has an average light yield for cosmic rays of 70 ± 10 photoelectrons. The light output from both sides of the detector and the total output spectra for cosmic rays are shown in Fig. 4. The dependence of the light yield on the particle position of impact is presented in Fig. 5.

Table 3
Light yield of 25 cm long water Cherenkov detector for different wall coverings

Wall covering	Yield [rel. units]
5 mm Teflon	100%
2 component paint NE 561	52%
2 component paint NE 561 + 1 mm Teflon	63%
1 component paint NE 560	68%
Immobilon-P	121%

The light yield of the water detectors was calculated as described in Appendix A. For the test and the final versions of the detector we obtained 94 and 86 photoelectrons, respectively (the reflectivity of Teflon was taken from Ref. [5]). Both values are slightly higher than the measured ones: 82 and 70.

An ideal threshold Cherenkov detector should have a 100% and zero efficiency for particles above and below the threshold respectively. We tested the detector efficiency for particles below threshold using protons with momenta analyzed by the magnetic spectrometer SPES 3 at SATURNE. The efficiency was below 1% and did not depend on the wavelength shifter addition.

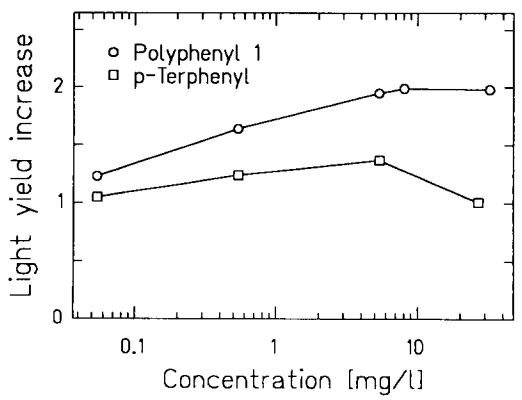

Fig. 6. Light yield increase in the water Cherenkov detector (25 × 10 × 10 cm^3) caused by the wavelength shifter addition as a function of the wavelength shifter concentration.

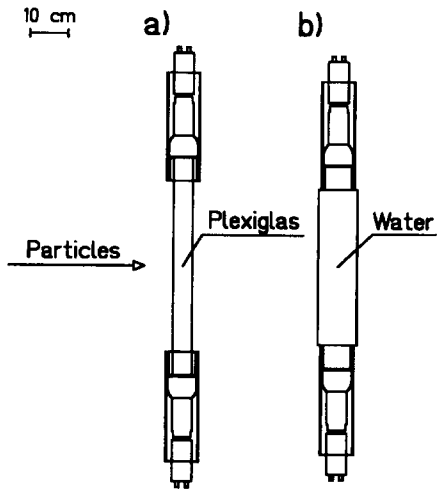

Fig. 7. Lucite and water Cherenkov detectors for KaoS. Both detectors have an active surface of 40×10 cm^2 and are read out at both ends with 3 in. photomultipliers. The average light yield for cosmic rays of the lucite and water detectors is 35 and 70 photoelectrons respectively.

3. Technical layout

The lucite and water Cherenkov detectors are presented in Fig. 7. All modules have an active area of 40×10 cm^2. The light produced in the radiators is detected by two 3 in. photomultipliers EMI 9821B mounted at the top and the bottom. The photomultipliers are shielded from the magnetic field by 0.7 mm thick permalloy and 3 mm thick soft-iron pipes. The shielding pipes protrude to protect the photocathode. The two photomultiplier signals are summed up and fed into a discriminator. The logical signal from it is used in the trigger logic.

The radiator of the lucite Cherenkov detector (Fig. 7a) is made of Plexiglas GS 218 [7] with a refraction index of 1.49. The lucite radiator is 40 cm high, 10 cm wide and 5 cm thick. The width is reduced at both ends in order to fit into the shielding pipe and to guide the light to the photomultiplier window. The radiator is wrapped in 8 layers of 0.1 mm Teflon and several layers of black light-tight tape. A 2 mm thick silicon pad is used as interface between the lucite radiator and the photomultiplier window. The detectors are calibrated by means of a nitrogen laser (wavelength $\lambda = 337$ nm). The laser light is transported via a light guide fiber which is coupled to the lucite radiator at the middle of the detector.

The water Cherenkov detector (Fig. 7b) is a $40 \times 10 \times 10$ cm^3 aluminum container with 2 mm wall thickness, filled with deionized water with an addition of 8 mg/l Polyphenyl 1 [13]. The walls are covered from inside with a Immobilon-P Transfer Membrane [12]. Two water filled cylinders guide the Cherenkov light from the detector to the photomultipliers. Each of them has a window made of UV transparent lucite. A silicon pad is used as interface between this window and the photomultiplier. Two steel pipes with a diameter of 5 mm at the top of the detector can be used to fill the detector with water. The rubber balls closing the pipes allow for an expansion of the water due to temperature changes. Through a hole in one of them a light guide fibre of the laser calibration system is inserted.

4. Performance and conclusions

We used pions and protons with momenta analyzed by the spectrometer to measure the overall efficiency of the row of 10 lucite detectors as a function of velocity (Fig. 8). The velocity was calculated from the momentum and corrected for the energy loss in the TOF stop scintillators. The efficiency ε was determined as

$$\varepsilon = N_1/N_0, \tag{5}$$

where N_0 is the number of particles per velocity bin observed by the TOF stop detector in the part of the focal plane which is completely covered by the lucite detectors, and N_1 tells how many of these particles caused a signal above the discrimination threshold in any of the lucite Cherenkov detectors. The statistical

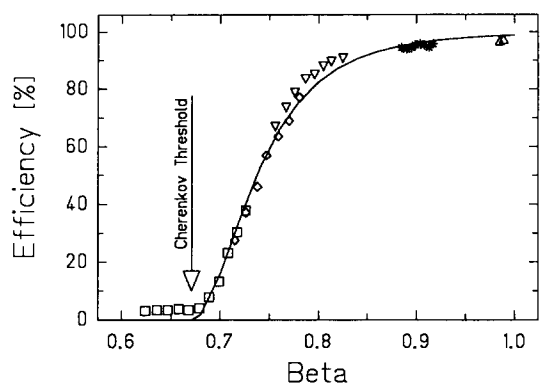

Fig. 8. The efficiency of the lucite Cherenkov detectors as a function of the particle velocity, measured with protons (squares and diamonds, corresponding to two magnetic field settings) and pions (triangles and stars) with momenta analyzed by the Kaon Spectrometer. The velocity was calculated from the momentum and corrected for the energy loss in the TOF stop scintillators. The solid line is the result of the two-parameter fit with the fit function given by Eq. (7) and the best fit parameters $N_{\mathrm{phe}}(1) = 14.3$ and $t_0 = 2.3$.

errors were calculated according to the binomial distribution:

$$\Delta\varepsilon = \sqrt{\varepsilon(1-\varepsilon)/N_0}. \tag{6}$$

The statistical errors are smaller than the symbol size in Fig. 8.

A two-parameter curve was fitted to the data points:

$$\varepsilon(\beta) = \exp(-N_{\mathrm{phe}}(\beta)) \sum_{i>i_0} \frac{(N_{\mathrm{phe}}(\beta))^i}{i!}, \quad \beta > 1/n, \tag{7}$$

where ε is the efficiency, $n = 1.49$ is the refraction index and $N_{\mathrm{phe}}(\beta)$ is the average number of photoelectrons for a particle with the velocity β:

$$N_{\mathrm{phe}}(\beta) = N_{\mathrm{phe}}(1)\ (1 - \frac{1}{n^2\beta^2}). \tag{8}$$

The mean number of photoelectrons for $\beta = 1$ particles $N_{\mathrm{phe}}(1)$ and the discrimination threshold i_0 are the fit parameters. The number $N_{\mathrm{phe}}(1)$ is responsible for the relative width of the light yield distribution and thus the steepness of the efficiency curve. The parameter i_0 determines the position where the efficiency curve goes through 50%.

The $N_{\mathrm{phe}}(1)$ value of 14.3 ± 0.2 obtained as a result of the fit is lower than the $N_{\mathrm{phe}} = 35 \pm 7$ measured for cosmic muons. This shows the difference between the detector performance under ideal conditions and in the practical application, where the position of impact, the incidence angle and the path length in the radiator differ from trajectory to trajectory. The obtained relative discrimination threshold $i_0/N_{\mathrm{phe}}(1) = 0.16 \pm 0.01$, on the other hand, agrees very well with the hardware thresholds set in the discriminators (typically between 0.15 and 0.20). The curve corresponding to these best fit parameters is shown in Fig. 8. The efficiency around $\beta = 0.8$ (open triangles) was determined using low momentum pions for which the correction for the energy loss in the TOF stop scintillators is largest ($\Delta\beta \approx -0.05$). The systematic difference between the data points and the fit curve in this region could be a sign that the assumption of the constant path length in the scintillators, used to calculate this correction, was oversimplified.

The lucite and water detectors were successfully used to suppress protons with momenta between 640 MeV/c and 1140 MeV/c at the trigger level. The discrimination threshold was at 15–20% of the $\beta = 1$ particle signal. The overall efficiency of the lucite/water detector row for pions, kaons and protons was 0.96, 0.86 and 0.02 respectively. In order to determine the kaon efficiency we simulated kaons by pions by decreasing the dipole magnetic field by a factor of 3.54, which is equal to the mass ratio m_K/m_π. This method is based on the assumption that the Cherenkov efficiency for $Z = 1$ particles depends only on velocity. Again, the difference between the velocity of kaons and pions which comes from the energy loss in the TOF stop scintillators, has to be taken into account.

In conclusion, lucite and water Cherenkov detectors, covering a large area (40 cm × 190 cm) behind the focal plane of the Kaon Spectrometer at SIS, could be successfully applied to suppress protons at the fast trigger level. A proton suppression factor of 50 was reached while the kaon efficiency was 86%.

This work was partly supported by the Polish Committee of Scientific Research under Contract NO. PB 201769101.

Appendix A. Cherenkov detectors – principle of operation

Charged particles passing through a medium loose energy mainly in collisions with electrons. The energy transfer to a given volume in the medium decreases exponentially with increasing distance from the particle trajectory. However, a different situation arises if the dielectric constant $\varepsilon(\omega)$ is real and the velocity of the particle is greater than the phase velocity of light in this medium in some ω range:

$$\beta > \beta_{\mathrm{ph}} = \frac{1}{\sqrt{\varepsilon(\omega)}}. \tag{A.1}$$

In such a case a certain amount of energy is radiated away as photons of frequency ω and with well defined emission angle Θ_C relative to the particle trajectory [14]:

$$\Theta_C = \arccos\left(\frac{1}{\sqrt{\varepsilon(\omega)}\beta}\right). \tag{A.2}$$

This effect is called Cherenkov radiation. The energy loss due to the Cherenkov effect per path length and frequency unit is given as

$$\left(\frac{\mathrm{d}E}{\mathrm{d}x\ \mathrm{d}\omega}\right)_C = \frac{(Ze)^2}{c^2}\omega\left(1 - \frac{1}{\beta^2\varepsilon(\omega)}\right), \tag{A.3}$$

where Ze is the charge of the particle [14]. In order to calculate the total energy loss due to the Cherenkov effect one has to integrate this expression over the whole frequency range for which $\varepsilon(\omega) < 1/\beta^2$.

The number of emitted photons, which is a more convenient variable than the energy loss, can be calculated from Eq. (A.3) as

$$\frac{\mathrm{d}N}{\mathrm{d}\lambda\ \mathrm{d}x} = \frac{2\pi\alpha Z^2}{\lambda^2}\left(1 - \frac{1}{\beta^2 n(\lambda)^2}\right), \tag{A.4}$$

where $\lambda = 2\pi c/\omega$ is the photon wavelength in vacuum and $n = \sqrt{\varepsilon}$ is the refraction index.

The Cherenkov threshold $\beta_C = 1/n(\lambda)$ and Cherenkov emission angle $\Theta_C = \arccos(1/\beta/n(\lambda))$ slightly depend on the wavelength of the observed photons. The factor $(1 - 1/\beta^2/n(\lambda)^2)$ is equal to $\sin^2\Theta_C$.

A standard Cherenkov detector consists of a radiator and a light collection and detection system. The light yield of a detector is usually expressed by the number of photoelectrons collected on the first dynodes of all photomultipliers coupled to the detector:

$$N_{\mathrm{phe}} = L \int_{\varepsilon(\lambda)>1/\beta^2} \eta_c(\lambda) q(\lambda) \epsilon(\lambda) \frac{\mathrm{d}N}{\mathrm{d}\lambda\,\mathrm{d}x}\,\mathrm{d}\lambda, \quad \text{(A.5)}$$

where λ is the photon wavelength in vacuum, $\eta_c(\lambda)$ is the collection efficiency of the first stage of the photomultiplier, $q(\lambda)$ is the quantum efficiency of the photocathode, $\epsilon(\lambda)$ is the light collection efficiency [1], L is the path length in the radiator and $\mathrm{d}N/\mathrm{d}\lambda\,\mathrm{d}x$ is the number of photons produced per unit path length and wavelength as given by Eq. (A.4).

The features of Cherenkov light can be summarized as follows:

(i) It is produced in transparent materials only if $\beta > \beta_C = 1/n(\lambda)$.

(ii) The photons are emitted at an angle Θ_C relative to the particle trajectory, $\cos(\Theta_C) = 1/\beta/n(\lambda)$.

(iii) The number of photons is proportional to Z^2 and increases from 0 at $\beta = \beta_C$ to its maximum at $\beta = 1$.

According to these properties three different types of Cherenkov detectors exist:

(i) Threshold Cherenkov detectors. The light is produced only when the particle velocity is above the threshold given by β_C. This allows a separation of particles according to their velocity. Particles with a defined momentum can be identified by this method. Such detectors are applied in the Kaon Spectrometer.

(ii) Ring Imaging Cherenkov Detector (RICH). Particle velocity and direction is determined by measuring the angle of emission of Cherenkov photons.

(iii) Detectors measuring the amount of produced light. It allows to determine the charge Z of the incident particle if its velocity is known.

Appendix B. Light yield calculation for the water Cherenkov detector

We calculated the expected light yield for the water Cherenkov detector without wavelength shifter in the following way: We divided the wavelength range from 180 nm to 700 nm in 10 nm wide bins. For each bin we calculated its contribution to the total light yield for $Z = \beta = 1$ particle:

$$\Delta N = L\eta_c(\lambda)q(\lambda)\epsilon(\lambda)\frac{2\pi\alpha}{\lambda^2}\left(1 - \frac{1}{n(\lambda)^2}\right)\Delta\lambda, \quad \text{(B.1)}$$

where λ is the mean wavelength in each bin, $\Delta\lambda$ is equal to 10 nm, $n(\lambda)$ is the refraction index and L the thickness of the radiator. The quantum efficiency $q(\lambda)$ for the photomultipliers EMI 9821B was taken from the THORN EMI photomultiplier handbook. The collection efficiency of the first dynode $\eta_c(\lambda)$ was assumed to be 0.8. The most crucial part of the calculation is the collection efficiency $\epsilon(\lambda)$. Our method to calculate the collection efficiency is based on the idea published in Ref. [15]. Additionally, we took into account the light absorption in water. It is important in our case because our detectors do not have separate light diffusion boxes and thus the photon paths in water can be quite long.

Lets consider a diffusion box with holes in the walls where the photomultipliers are mounted. The following statistical approach is correct if the relative area covered by the photomultiplier windows F is small compared to 1. The photons reaching the photocathode can be divided into groups, corresponding to the number of reflections:

$$\epsilon = \frac{1}{N_0}\sum_{k=0}^{\infty} N(k)Ft, \quad \text{(B.2)}$$

where N_0 is the number of produced photons, and $N(k)$ is the numbers of photons which survived k reflections without being absorbed by walls, medium or photomultipliers. F is the probability that a photon reaches the photomultiplier window, whereas the transmission t denotes the probability that the photon goes through the window and reaches the photocathode. The number of photons decreases after each reflection by a factor R:

$$R = N(k+1)/N(k) = \langle r\rangle A, \quad \text{(B.3)}$$

$$\langle r\rangle = (1-F)r + F(1-t), \quad \text{(B.4)}$$

$$A = \exp(-\langle s\rangle/\Lambda), \quad \text{(B.5)}$$

where $\langle r\rangle$ is the reflection coefficient averaged over the walls (reflectance r) and the photomultiplier windows (reflectance $1 - t$). A is the factor responsible for absorption of photons in the medium with the absorption length Λ. The mean path length between two subsequent reflections $\langle s\rangle$ for the diffusing box of dimensions $W \times W \times H$ was taken from Ref. [16]:

$$\langle s\rangle = \frac{1}{2W^2 + 4WH} \times \left(\pi W^2 H + \frac{WH}{\sqrt{1 - 4/\pi^2}}\sqrt{H^2 + W^2}\right). \quad \text{(B.6)}$$

[1] Light collection efficiency $\epsilon(\lambda)$ is defined as the probability that a photon of wavelength λ produced in the radiator hits the photocathode of a photomultiplier.

Thus the number of photons which survive k reflections and traverse an average length in the medium equal to $(k + 0.5)\langle s\rangle$ is

$$N(k) = N_0\sqrt{A}R^k . \tag{B.7}$$

The collection efficiency is

$$\epsilon = \sum_{k=0}^{\infty} Ft\frac{N(k)}{N_0} = Ft\sqrt{A}\sum_{k=0}^{\infty} R^k = \frac{Ft\sqrt{A}}{1-R}, \tag{B.8}$$

$$\epsilon = \frac{Ft\exp(-\langle s\rangle/2\Lambda)}{1-\langle r\rangle\exp(-\langle s\rangle/\Lambda)} . \tag{B.9}$$

The value of ϵ depends on λ through $\langle r\rangle, \Lambda$ and t. Without absorption in the medium ($\Lambda \to \infty$) this expression reduces to

$$\epsilon = \frac{Ft}{1-\langle r\rangle}, \tag{B.10}$$

published in Ref. [15][2].

The mean path length of photons $\langle S\rangle$ and its variance σ_S^2 can be calculated in the following way:

$$\begin{aligned}\langle S\rangle &= \langle s\rangle\frac{\sum_{i=0}^{\infty} N(i)(i+0.5)}{\sum_{i=0}^{\infty} N(i)} \\ &= \langle s\rangle\left(0.5 + \frac{\sum_{i=0}^{\infty} iR^i}{\sum_{i=0}^{\infty} R^i}\right) \\ &= \langle s\rangle\left(0.5 + \frac{R}{1-R}\right), \end{aligned} \tag{B.11}$$

$$\begin{aligned}\sigma_S &= \langle s\rangle\sqrt{\frac{\sum_{i=0}^{\infty} R^i(i+0.5)^2}{\sum_{i=0}^{\infty} R^i} - \left(0.5 + \frac{R}{1-R}\right)^2} \\ &= \langle s\rangle\frac{\sqrt{R}}{1-R} . \end{aligned} \tag{B.12}$$

The standard deviation σ_S can be used to calculate the contribution of the light collection system to the duration of the detector signal.

The calculation yields a light collection efficiency of 30% and a mean photon path length $\langle S\rangle$ of 50 cm for photons of $\lambda = 400$ nm in the test detector described in Section 2.3. The calculated total light yield ($N_{\mathrm{phe}} = 94$) agrees relatively well with the measured one ($N_{\mathrm{phe}} = 82$).

References

[1] R.Stock, Phys. Rep. 132 (1986) 259.
[2] J. Aichelin and Che Ming Ko, Phys. Rev. Lett. 55 (1985) 2661.
[3] P. Senger et al., Nucl. Instr. and Meth. A 327 (1993) 393.
[4] D. Brill et al., Phys. Rev. Lett. 71 (1993) 336.
[5] C.R. Bower et al., Nucl. Instr. and Meth. A 252 (1986) 112.
[6] Nuclear Enterprises Limited, Bath Road, Beenham, Reading RG7 5PR, England.
[7] Röhm GmbH Chemische Fabrik, Kirschenallee, D-6100 Darmstadt, Germany.
[8] E.J. Sacharidis, Nucl. Instr. and Meth. 101 (1972) 327.
[9] Thorn EMI Electron Tubes Ltd., Bury Street, Ruislip Middlesex HA4 7TA England.
[10] P.H. Garbincius, Nucl. Instr. and Meth. 131 (1975) 273.
[11] S.P. Ahlen et al., Nucl. Instr. and Meth. 136 (1976) 235.
[12] Millipore GmbH, Hauptstr. 87, D-6236 Eschborn, Germany.
[13] Lambda Physik GmbH, Hans-Boeckler-Str. 12, D-3400 Göttingen, Germany.
[14] J.D. Jackson, Classical Electrodynamics (Wiley, New York, 1975).
[15] M.H. Salamon and G. Tarlé, Nucl. Instr. and Meth. 161 (1979) 147.
[16] S.P. Ahlen, Ph.D Thesis, University of California, Berkeley (1976).

[2] There is a printing error in the corresponding formula in Ref. [15].